Received: 2 March 2022 | Revised: 29 March 2022 | Accepted: 1 April 2022

DOI: 10.1002/btpr.3255

RESEARCH ARTICLE

Bioseparations and Downstream Processing

BIOTECHNOLOGY PROGRESS

Effect of filtrate flux and process disruptions on virus retention by a relatively homogeneous virus removal membrane

Mohammad A. Afzal | Andrew L. Zydney

Department of Chemical Engineering, The Pennsylvania State University, University Park, Pennsylvania, USA

Correspondence
Andrew L. Zydney, Department of Chemical Engineering, The Pennsylvania State University, University Park, PA 16802, USA.
Email: zydney@engr.psu.edu

Funding information
NSF IUCRC program, Grant/Award Number: 1841474

Abstract

Recent studies have shown that virus retention by specific virus filters can be reduced at low flow rates and after process disruptions; however, the magnitude of these changes in virus retention and the underlying mechanisms controlling this behavior are still not well understood. The objective of this study was to develop a quantitative understanding of the factors controlling the virus retention behavior of a relatively homogeneous polyvinylidene fluoride virus removal filter. Data were obtained with the bacteriophage ϕX174 as a model virus. Virus retention decreased as the filtrate flux was reduced and also declined slightly over the course of the virus filtration. Virus retention immediately after a process disruption decreased by as much as a factor of 1000 (3-logs) depending on the duration and timing of the disruption. The experimental results were well-described using an internal polarization model that accounts for accumulation and release of virus during the filtration / disruption, with the key model parameters dependent on the filtrate flux. These results provide important insights into the factors controlling the virus retention behavior as well as guidelines for the effective use of virus removal filters in bioprocessing.

KEYWORDS
monoclonal antibody, process disruption, virus filtration, virus retention

1 | INTRODUCTION

Virus filtration plays a crucial role in the removal of both adventitious and exogenous viruses in the production of plasma-derived and animal cell-based biotherapeutics. Viral contamination by the adventitious parvovirus minute virus of mice (MVM) has been reported by Kiss,[1] and it is well known that endogenously expressed retrovirus-like particles are frequently released by many CHO cell lines.[2] The various international regulatory agencies recommend the use of at least two orthogonal steps involving different mechanisms of viral clearance as part of the downstream process.[3,4] Virus filtration can provide a robust size-based removal of both enveloped and non-enveloped viruses.

Several studies have identified conditions where the virus removal capability of particular virus filters becomes compromised, including operation at high volumetric throughput,[5–7] low filtrate flux,[8–10] and in response to a process disruption.[11–14] However, the underlying mechanisms governing the loss of virus retention are still unclear. For example, Bolton et al[5] attributed the decline in virus transmission at high throughput to selective plugging of small pores, while Jackson et al[7] hypothesized that this behavior was due to the development of internal virus polarization of retained virus within the more open region of the virus filter. LaCasse et al[15] attributed the loss in virus retention at low pressure to internal diffusion within the virus filter, with the low convective flow allowing the virus to diffuse around pore constrictions, thereby increasing the probability of virus transmission through the membrane. Yamamoto et al[10] reported similar behavior for the Planova 20N membrane, although they described the loss in retention due to the relative contributions of hydrodynamic and Brownian forces on the capture of virus at low versus high flow rates.

The decrease in virus retention after a process disruption[11–14] has typically been attributed to the diffusion of viruses within the virus filter in the absence of any pressure-driven flow. This is consistent with the greater increase in virus transmission seen after longer disruption times.[15,16] However, Woods and Zydney[14] also found that there was a significant, although slightly less pronounced, increase in virus transmission when the pressure was rapidly decreased from 210 kPa to a small (but non-zero) pressure. However, no quantitative description has been developed to describe the effects of disruption time and the magnitude of the pressure disruption on virus retention.

The objective of this study was to develop a more complete understanding of the virus retention behavior of a relatively homogeneous polyvinylidene fluoride membrane (PVDF) virus removal membrane, used in the Pegasus™ SV4 virus filter, under different flow conditions and in response to different process disruptions. Data were obtained with the bacteriophage ϕX174, which is 26 nm in size with an icosahedral shape, as a model virus. ϕX174 has been used previously as a surrogate for mammalian viruses like MVM due to their similar size (approximately 25 nm) and surface charge. The experimental results were analyzed using an internal virus polarization model, extended to account for the time-dependent release of virus during a process disruption and the presence of two parallel retention zones. These results provide insights into the factors controlling virus retention as well as guidelines for the effective use of virus filters in bioprocessing.

2 | MATERIALS AND METHODS

2.1 | Bacteriophage and host bacterial cell

Escherichia coli (ATCC-13706) and bacteriophage ϕX174 (ATCC-13706-B1) were obtained from the American Type Culture Collection (ATCC, Manassas, VA). Colonies of the *E. coli* host were isolated by streak-plating and incubated in Difco Nutrient Broth (NB) media (8 g/L, BD-234000) at 37°C until reaching an optical density of 0.3–0.4 (evaluated at 600 nm). The solution was then spiked with 100 μl of a high titer phage suspension (~10^9 pfu/ml) and incubated in a G24 Environmental Incubator Shaker (New Brunswick Scientific, Edison, NJ) for approximately 6 h under gentle agitation. The resulting lysate was purified by centrifugation at 3500 rpm for 10 min in a Beckman Coulter centrifuge (Brea, CA), with the supernatant collected and re-centrifuged two additional times. The bacteriophage suspension was then passed through a 0.2 μm nominal pore size syringe filter (VWR International, Radnor, PA) and stored at 4°C.

Phage concentrations were evaluated using a plaque-forming assay conducted on agar plates made with NB media (8 g/L), NaCl (5 g/L from Promega Corp., Madison, WI), and Difco agar (15 g/L, BD-214530) mixed in deionized water. A volume of 100 μl of a bacteriophage sample and 200 μl of *E. coli* were mixed with 3 ml of a soft agar solution (5 g/L agar) and poured over the solidified agar plate. The plate was inverted and incubated at 37°C for 6–8 h. The phage infected and lysed the *E. coli*, with the region of lysed cells visible as a plaque. The plaques were counted, with the phage titer reported as the number of plaque-forming units/ml (pfu/ml). Bacteriophage samples were run in replicate, with the concentration determined from serial dilutions performed to obtain between 5 and 200 plaques per plate. All procedures were performed under aseptic conditions in a Purifier Logic+ Class II, Type AS Biosafety cabinet (Labconco Corp, Kansas City, MO).

2.2 | Virus filtration

Virus filtration was performed using a single layer of a hydrophilized PVDF virus removal filter having a nominal pore size rating of 20 nm and a thickness of approximately 30 μm. The membrane was relatively homogeneous (symmetric), with the pore size and pore density being relatively uniform through the depth of the filter.[18] The membrane was provided by Pall Corporation (FTKSV4047025; Port Washington, NY) as two layers of 47 mm diameter discs as part of the Pegasus™ SV4 virus removal filter. A small 25 mm disc was prepared using a specially-designed cutting device and immersed in deionized water to carefully separate the layers. A single layer of membrane was then placed with the shiny side facing downstream (away from the feed flow, as per the orientation in the dual layer Pegasus™ SV4 virus removal filter) in a 25 mm polypropylene filter holder (43303010; Advantec MFS, Inc., Dublin, CA) having a filtration area of 3.5 cm^2. Experiments were performed with only a single layer of membrane to make it easier to detect the phage in the permeate samples and to facilitate modeling.

Filtration experiments were performed at constant filtrate flux maintained by a peristaltic pump (Masterflex, Vernon Hills, IL) placed upstream of the filter capsule. The filter was initially flushed with at least 70 L/m^2 of a solution containing 10 mM phosphate buffer with 137 mM NaCl and 2.7 mM KCl at pH 7.4 (PBS). The feed reservoir was then filled with a bacteriophage suspension, using approximately 10^8 pfu/ml in PBS. The transmembrane pressure was evaluated using an Ashcroft Digital Pressure gauge (Stratford, CT). Grab samples of 0.6 ml were collected throughout the filtration, with 0.15 ml samples collected immediately after any process disruption. Data were analyzed in terms of the log reduction value (LRV) for small grab samples:

$$\mathrm{LRV} = -\log_{10}\left(\frac{C_{\mathrm{filtrate}}}{C_{\mathrm{Feed}}}\right) \quad (1)$$

where C_{filtrate} and C_{Feed} are the ϕX174 concentrations in the filtrate and feed samples, respectively.

3 | RESULTS AND DISCUSSIONS

3.1 | Filtration without disruption

Figure 1 shows typical data for the LRV for ϕX174 filtration through a single layer of the PVDF membrane evaluated from small grab

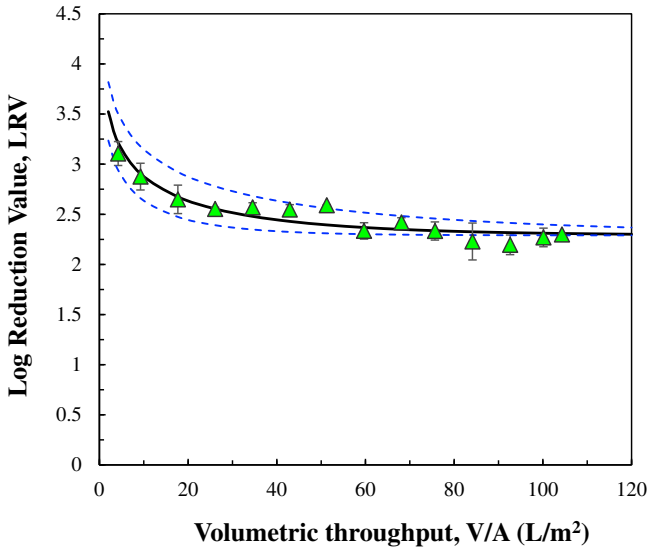

FIGURE 1 Virus retention for the polyvinylidene fluoride membrane at a constant filtrate flux of 50 L/m^2/h. The solid curve represents the best fit using the internal polarization model (Equation 4), while the dashed curves are the model calculations with twofold higher and lower sieving coefficients as described in the text. The error bars on the data points represent plus / minus one standard deviation

samples obtained during an experiment performed at a constant filtrate flux of 50 L/m^2/h. Note that limited experiments performed with two layers of the PVDF membrane showed no detectable ϕX174 in the permeate samples, consistent with an LRV that is twice that for the single layer membrane. The data are plotted as a function of the volumetric throughput (cumulative filtrate volume normalized by the membrane area). The symbols represent the average of replicate measurements, with the error bars showing the standard deviation. The transmembrane pressure remained nearly constant over the course of the filtration, increasing slightly from 127 to 134 kPa, suggesting that there was minimal membrane fouling during the constant flux filtration of the ϕX174 suspension; any fouling seen during the experiment would have caused a reduction in permeability and an increase in transmembrane pressure. In contrast, the LRV declined slowly over the course of the filtration, decreasing from a value of 3.1 in the initial grab sample to a value of 2.3 after 100 L/m^2, corresponding to more than a sixfold increase in virus concentration in the filtrate samples. A similar decrease in LRV during constant flux filtration through the Pegasus™ SV4 was reported by David et al[17] using a very low flux of 0.3 L/m^2/h, with the LRV decreasing to nearly zero after only 15 L/m^2 under those conditions.

The reduction in virus retention during filtration through the Ultipor DV20 membrane, which has a relatively homogeneous pore structure similar to the hydrophilized PVDF membrane used in the current study, has previously been analyzed using an internal concentration polarization model that accounts for the accumulation of virus within the entrance region of the membrane.[7] A simple mass balance on mobile virus was written as:

$$V_R \frac{dC}{dt} = xqC_F - qSC \tag{2}$$

where C and C_F are the virus concentrations in the reservoir zone and feed, respectively, and V_R is volume of the reservoir zone. The virus that enter the filter can either be irreversibly captured, for example, within a highly constricted pore region within the membrane, or they can accumulate in the reservoir zone. The parameter x is the fraction of virus entering the reservoir zone that accumulate in the reservoir zone (i.e., the fraction of virus that remain mobile), while $1-x$ is the fraction of virus that are captured. At any instant in time, a small fraction of the virus that accumulate in the reservoir zone are transported into the collected filtrate, with this fraction described by the sieving coefficient, S. Equation (2) can be directly integrated to give:

$$C = \frac{C_F x}{S}[1 - \exp(-SV/V_R)] \tag{3}$$

where V is cumulative volumetric throughput and the virus filter is assumed to be filled with virus-free buffer at the start of the experiment. The LRV is thus given as:

$$\mathrm{LRV} = -\log_{10} x - \log_{10}[1 - \exp(-\mathrm{SV}/V_R)] \tag{4}$$

where the virus concentration in the filtrate is simply equal to S^*C. Equation (4) is valid for a single layer membrane; Jackson et al[7] have discussed the extension of the model to a multi-layer membrane. The solid curve in Figure 1 is developed using $x = 0.0051$ and $S = 1.2 \times 10^{-4}$ as determined by minimizing the sum of the squared residuals between the model and data, with $V_R/A = 0.004$ L/m^2 based on the 8 μm thickness of the capture (reservoir) zone in confocal images obtained by Leisi et al[18] showing fluorescently-labeled virus in a narrow band near the feed size of the membrane (where V_R/A is calculated assuming a membrane porosity of 50%). The parameter S determines the rate at which the virus accumulate in the reservoir zone, and thus the rate at which the LRV declines, with the virus concentration within the reservoir zone approaching a value of $C_F x/S$ at large volumetric throughput. The model calculations are relatively insensitive to small changes in S, as shown by the dashed curves in Figure 1 (constructed using $S = 0.6 \times 10^{-4}$ and 2.4×10^{-4}, two-fold lower and higher than the best fit value). In contrast, the model calculations are very sensitive to the best fit value of x, with Equation (4) giving $\mathrm{LRV} = -\log_{10} x$ at large V/A, irrespective of the value of the sieving coefficient. At this point the concentration of mobile virus within the reservoir zone approaches its steady-state value, with the concentration of virus in the reservoir zone predicted to be approximately 40 times that in the feed based on the best fit values of the parameters determined from the data in Figure 1.

Further confirmation of the internal polarization model was obtained by challenging the PVDF membrane with 39 L/m^2 of the ϕX174 suspension (corresponding to 1.4×10^7 total pfu) with the feed then switched to PBS for the next ~1700 L/m^2 using a trivalve without any disruption in the filtrate flux. The experiment was performed

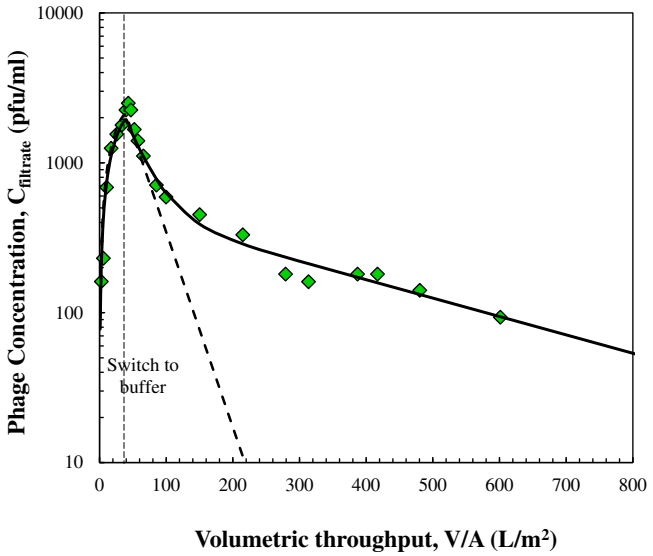

FIGURE 2 Virus concentration in filtrate samples as a function of volumetric throughput for an experiment in which the polyvinylidene fluoride membrane was challenged with ϕX174 for 39 L/m^2 followed by a virus-free buffer flush. The dotted vertical line shows the point where the feed was switched to buffer. The dashed and solid curves represent the model calculations using the one and two-reservoir models, respectively

at a constant filtrate flux of 50 L/m^2/h, corresponding to a total filtration time of more than 36 h. Results for the ϕX174 concentration in the filtrate samples over the first 800 L/m^2 of this experiment are shown in Figure 2. The ϕX174 concentration increases rapidly during the virus challenge, going from 160 to 1800 pfu/ml, due to the accumulation of virus within the reservoir zone. There is a relatively rapid (approximately fivefold) decay in ϕX174 concentration over the first 50 L/m^2 of buffer flush followed by a much slower decrease to a value of 30 pfu/ml after 1730 L/m^2 of buffer (beyond the scale shown in Figure 2), which corresponds to a total buffer volume nearly 50 times the volume of feed filtered during the initial virus challenge. Note that the total number of ϕX174 in the initial challenge was 1.4 x 10^7 pfu, with less than 0.1% of these virus collected in the initial 39 L/m^2 (during the phage challenge) and then an additional 0.6% of the initial challenge collected during the 1730 L/m^2 buffer flush; more than 99% of the ϕX174 remain captured within the virus filter. This behavior has not been reported previously since the virus concentration in permeate samples obtained during a subsequent buffer flush have only been evaluated for relatively small filtrate volumes.

The dashed curve in Figure 2 represents the model calculation given by the simple internal polarization model, with the decay in concentration during the buffer flush evaluated by integrating Equation (2) without the input term giving:

$$\frac{C}{C^*} = \exp\left[-\frac{S(V-V^*)}{V_R}\right] \tag{5}$$

where V^* is the volumetric throughput used for the virus challenge and C^* is the virus concentration in the reservoir zone at the start of the buffer flush (evaluated from Equation 3 at $V = V^*$). The dashed curve was obtained using $S = 1.2 \times 10^{-4}$ (the value determined for the data in Figure 1) with the best fit value of $x = 0.0030$ determined by minimizing the sum of the squared residuals between the model and data over the first 50 L/m^2. The slightly smaller value of x determined from this data set likely reflects the inherent membrane-to-membrane variability in virus capture. The model calculations were in good agreement with experimental data for the initial phage challenge and for the first 40 L/m^2 of the buffer flush. However, the model significantly over-predicts the rate at which the virus are cleared from the filter, with the ϕX174 concentration predicted to drop below 10 pfu/ml after only 180 L/m^2 of buffer.

Although it is possible to obtain a somewhat better fit to the data during the buffer flush using a smaller value of S, Equation (5) is unable to explain the bi-phasic decay in virus concentration seen in Figure 2. Instead, the data suggest that there might be multiple pathways involved in the accumulation / transmission of virus during the buffer flush. This was described mathematically by rewriting Equation (2) for two separate reservoir zones as:

$$V_{Ri}\frac{dC_i}{dt} = x_i q_i C_F - q_i S_i C_i \tag{6}$$

For simplicity, we assumed that the flow partitions equally into each zone based on the reservoir volume, that is,

$$f_i = \frac{V_{Ri}}{V_R} = \frac{q_i}{q} \tag{7}$$

where V_R and q are the total reservoir volume and total filtrate flow rate, respectively. In addition, we assumed that virus capture was equal in both zones, that is, $x_1 = x_2 = x$. Under these conditions, the virus concentration in the filtrate stream during the buffer flush is given as:

$$C = fC_1^* S_1 \exp\left[-\frac{S_1(V-V^*)}{V_R}\right] + (1-f)\,C_2^* S_2 \exp\left[-\frac{S_2(V-V^*)}{V_R}\right] \tag{8}$$

where S_1 and S_2 are the virus sieving coefficients for the two compartments, C_1^* and C_2^* are the concentrations in the two compartments at the end of the virus challenge (both evaluated from Equation 3), and f is the fraction of the flow (and volume) in reservoir 1. The solid curve in Figure 2 is based on Equation (8) with $f = 0.33$, $x = 0.0063$, and $S_2 = 1.1 \times 10^{-5}$, again using $S_1 = 1.2 \times 10^{-4}$. The resulting double exponential fit is in very good agreement with the experimental data throughout the buffer flush. This bi-phasic behavior may represent inhomogeneities in the virus filter, with regions having smaller and larger pores (and thus sieving coefficients), although additional studies would be required to validate the underlying physics of this two-compartment model for virus capture in the PVDF membrane.

Further insights into the virus capture behavior of the PVDF virus filtration membrane were obtained by challenging the filter with 35 L/m^2 of the ϕX174 suspension and then flushing the filter with buffer but in the opposite direction of the challenge. Multiple samples were obtained throughout the 2100 L/m^2 buffer flush, with the ϕX174 recovery evaluated by integration of the virus concentration data over the collected volume. More than 60% of the phage in the initial challenge were released during this reverse buffer flush experiments, which is approximately 100 times greater than the number of virus recovered during the forward buffer flush, demonstrating that most of the virus are strongly captured within the membrane pore structure (in the absence of backflushing).

3.2 | Process disruptions

The effects of multiple process disruptions on virus retention by the PVDF membrane is examined in Figure 3. The experiment was performed at a constant filtrate flux of 50 L/m^2/h using a ϕX174 concentration of 2.2 x 10^6 pfu/ml. Ten-min disruptions (with zero flow) were introduced at volumetric throughputs of 38, 74, and 109 L/m^2, with the ϕX174 concentration evaluated in permeate samples obtained throughout the experiment. The LRV decreases during the initial virus challenge, similar to the results in Figure 1. The measured LRV immediately after the process disruptions were all around zero, that is, the virus concentration in the first permeate samples obtained after the process disruption was nearly identical to the virus concentration in the feed and increased even further after the subsequent disruptions. The similar response after each disruption clearly indicates that there was no damage to the PVDF membrane, with the LRV returning to a value of approximately 2.3 within 25 L/m^2 after re-starting the filtration. Similar results were obtained in experiments in which three separate membrane disks were challenged to the three different throughputs followed by a single process disruption.

The solid curve in Figure 3 is developed using the modified internal polarization model developed by Woods and Zydney[14] which assumes that some fraction (y) of the previously captured virus are released during the process disruption. These released virus can either be recaptured after re-starting the filtration or they can pass into the permeate solution, with the concentration of these released virus (C_r) given as:

$$C_r = \frac{y(1-x)V^* C_{\text{Feed}}}{V_R}\left[1-\exp\left(-\frac{(S+z)(V-V^*)}{V_R}\right)\right] \quad (9)$$

where z describes the rate at which the released virus are recaptured and V^* is the volumetric throughput at which the disruption occurred. The virus concentration in the filtrate is given by the sum of the virus that are transmitted from the reservoir and those that were released during the process disruption:

$$C_{\text{filtrate}} = S*C + S*C_r \quad (10)$$

The solid curve was obtained with $x = 0.0095$, $z = 0.0040$, and $y = 0.51$ with $S = 1.2 \times 10^{-4}$ as previously determined. The model calculations are again in very good agreement with the experimental data, demonstrating that the modified internal polarization model is able to effectively describe the virus retention behavior after a process disruption.

An additional process disruption experiment was performed using a 38 L/m^2 virus challenge followed by a 10 min disruption and then a buffer flush with results shown in Figure 4. The ϕX174 concentration

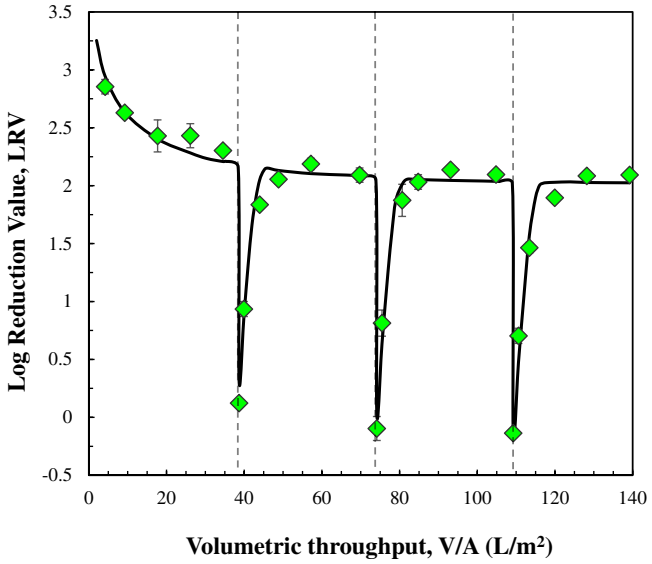

FIGURE 3 Effect of process disruptions on LRV. Data obtained at a filtrate flux of 50 L/m^2/h with 10 min disruptions at 38, 74, and 109 L/m^2 as shown by the vertical dashed lines. Solid curve is model calculation as described in the text

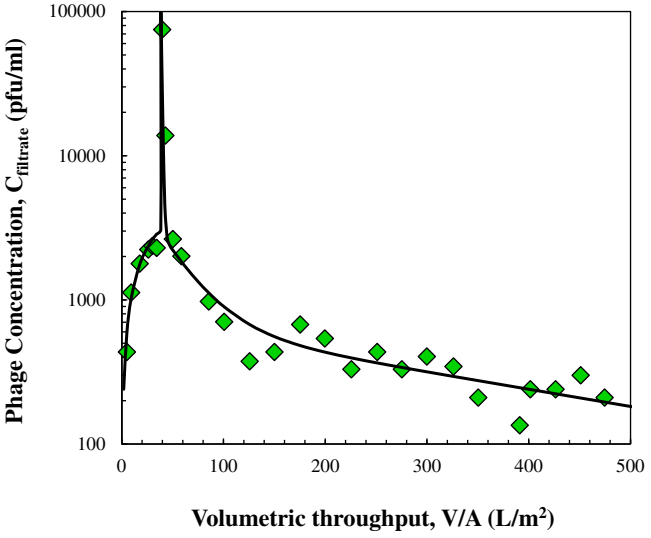

FIGURE 4 Virus concentration in the filtrate samples as a function of volumetric throughput for an experiment in which the polyvinylidene fluoride membrane was challenged with the ϕX174 for 35 L/m^2 followed by a 10 min disruption and then a virus-free buffer flush. The solid curve is the model fit as described in the text

increased by nearly two orders of magnitude after the disruption but then decreased quite rapidly before decaying more slowly at larger volumetric throughput. The solid curve is the model fit determined using the same values of S_1, S_2, and f determined from the data in Figure 2 and the same values of y and z as determined in Figure 3 for both compartments; the only parameter fit to the data in Figure 4 was $x = 0.013$. The two-compartment internal polarization model was able to effectively describe the increase in virus concentration after the process disruption as well as the decay during the buffer flush. Note that it would have been possible to obtain somewhat better agreement with the data by fitting additional parameters (instead of using the previously determined values), although this was not justified given the very good fit seen in Figure 4.

Figure 5 shows results from a series of experiments performed with process disruptions varying from 2 to 20 min in duration, all for constant flux filtration experiments at 50 L/m^2/h after an initial volumetric throughput of 36 L/m^2. The virus transmission increases immediately after the disruption, with the change in LRV being greatest for the experiment performed with the longest disruption time. This behavior is consistent with the greater time for virus diffusion out of the pores as discussed by Lacasse et al.[15] The change in LRV increases from 0.9 logs (a factor of 7.9) to 2.8 logs (nearly a factor of 1000) as the disruption time increases from 2 to 20 min. The solid curves in Figure 5 are model calculations with $S = 1.2 \times 10^{-4}$ and $z = 0.004$, based on the results in Figures 1–4, with the best fit value of $x = 0.0047$. The best fit values of y were determined separately for each disruption time with values summarized in Table 1. The 2 min disruption only provides sufficient time for about 3% of the previously captured virus to diffuse out of the pores, while the model indicates that all of the virus are released after a 20 min disruption ($y = 1$).

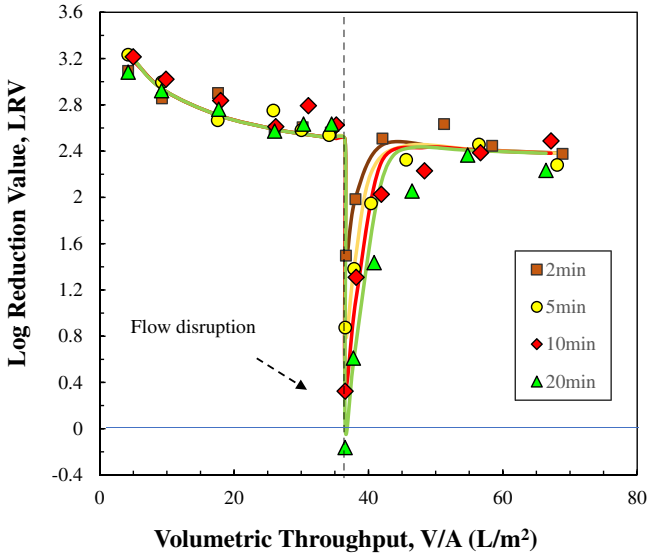

FIGURE 5 Effect of process disruption time on virus retention. Data obtained with ϕX174 at a concentration of 3 x 10^6 pfu/ml at a constant flux of 50 L/m^2/h with disruptions at a volumetric throughput of 36 L/m^2. Solid curves are model calculations with parameters given in Table 1

In order to confirm that the effects seen in Figure 5 were not due to small filter-to-filter differences in the PVDF membrane, a separate experiment was performed using a single membrane but with multiple disruptions occurring sequentially (with different disruption times), in each case allowing the virus transmission to first return to its "stable" value. The virus retention behavior during this sequential disruption experiment is shown in Figure 6, with the solid curve developed using the same values of *S* and *z* with the best fit values of *x* and *y* given in Table 1. The fraction of captured virus released during the process disruption for this sequential disruption experiment again increases with increasing disruption time, with values that are very similar to those determined previously from experiments performed with the four separate membranes each subjected to a single process disruption (Figure 5).

3.3 | Filtrate flux effects

All the data in Figures 1–6 were obtained at a constant filtrate flux of 50 L/m^2/h (50 LMH). The effect of the filtrate flux on virus retention

TABLE 1 Best fit values of the fraction of virus that are not captured by the PVDF membrane (*x*) and the fraction of virus released during the process disruption (*y*) as a function of the disruption time for both separate and sequential process disruptions at a filtrate flux of 50 L/m^2/h determined with $S = 1.2 \times 10^{-4}$ and $z = 0.004$

Disruption duration (min)	*y* (Separate)	*y* (Sequential)
2	0.03	0.03
5	0.16	0.18
10	0.41	0.58
30	1	1
x	0.004	0.010

Abbreviation: PVDF, polyvinylidene fluoride membrane.

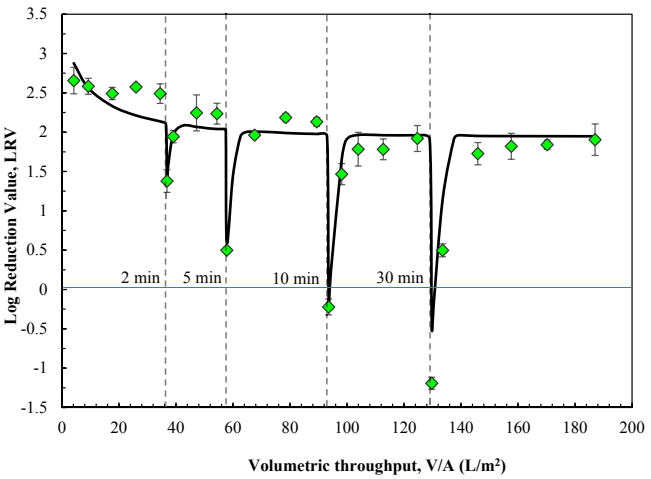

FIGURE 6 Effect of multiple sequential process disruptions on virus retention. Data obtained at a filtrate flux of 50 L/m^2/h with disruptions of 2, 5, 10, and 30 min duration as shown by dashed vertical lines. Solid curve is the model calculation using parameters given in Table 1

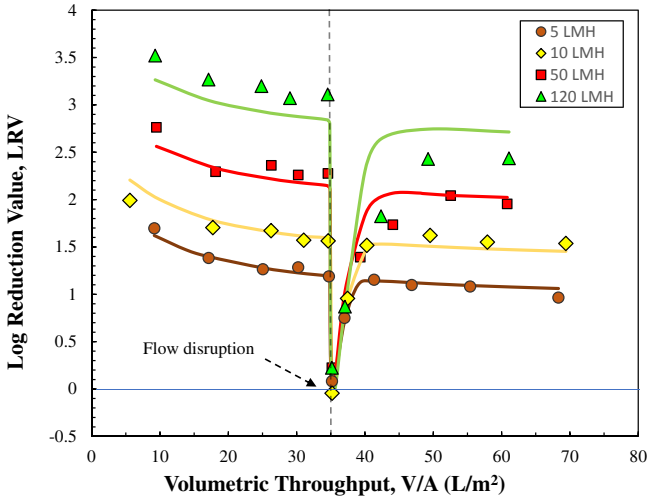

FIGURE 7 Effect of process disruption on the virus retention at different filtrate flux. Data obtained with a 10 min disruption at a volumetric throughput of approximately 35 L/m^2 as denoted by the dashed vertical line. Solid curves are model calculations using the parameter values given in Table 2

is examined in Figure 7. Results are shown from a series of experiments performed at different filtrate flux (from 5 to 120 L/m^2/h), each with a separate membrane for which a 10 min process disruption was imposed after a volumetric throughput of 35 L/m^2. The initial virus retention was a strong function of the filtrate flux, decreasing from LRV = 3.4 at 120 L/m^2/h to only LRV = 1.6 at 5 L/m^2/h. Note that Pegasus™ SV4 virus filter is typically run at high filtrate flux using two layers of the PVDF membrane, with the data in Figure 7 suggesting that such a configuration would provide an LRV of around six (twice the LRV of the single layer of PVDF membrane). The LRV during the first 35 L/m^2 (before the process disruption) declines with increasing volumetric throughput due to the accumulation of virus within the reservoir zone. The virus transmission increases dramatically immediately after the process disruption, with the LRV in the initial permeate sample being close to zero for all four experiments. Thus, the magnitude of the reduction in LRV is greatest at the highest filtrate flux (a change in LRV of more than 3-logs) and decreases to only slightly more than 1-log at a flux of 5 L/m^2/h. The LRV increases very rapidly in the first few samples obtained immediately after the disruption for the runs at low filtrate flux, but this increase in LRV occurs more slowly (over approximately 30 L/m^2) for the run at 120 L/m^2/h.

The solid curves in Figure 7 are the model calculations using $S = 1.2 \times 10^{-4}$ and $z = 0.004$, as determined previously, with the best fit values of y (assumed to be the same for all four experiments) and x (assumed to be a function of the filtrate flux) shown in Table 2. Although it was possible to get slightly better agreement with the data by fitting S, y, and / or z at each flux separately, there were no obvious trends in the resulting values. This suggests that the different LRV profiles before the process disruption are due entirely to differences in the probability that the virus is captured within the pore structure, with the fraction of captured virus (equal to $1 - x$) increasing from 90.1% at 5 L/m^2/h to 99.8% at 120 L/m^2/h. However, this change in

TABLE 2 Best fit values of the parameters x and y in the modified internal polarization model at the different filtrate flux

Flux (L/m^2/h)	x
5	0.099
10	0.040
50	0.011
120	0.002
y	0.99

x has relatively little effect on the measured LRV immediately after the process disruption, which can be approximated as:

$$\mathrm{LRV} = -\log_{10}\left[\frac{(1-x)ySV^*}{V}\right] \tag{11}$$

where we have neglected the contribution from the originally free (not captured) virus. Equation (9) gives LRV = 0.27 at 5 L/m^2/h and 0.21 at 120 L/m^2/h; these values would be even closer if one accounted for the slightly greater transmission of virus through the filter at the lower filtrate flux.

4 | CONCLUSIONS

The data presented in this study for virus capture by the PVDF virus removal membrane confirm results from several previous studies regarding the performance of virus filters, including the reduction in virus retention at low flow rates, after process disruptions, and with increasing volumetric throughput. The change in virus retention by the PVDF membrane after a process disruption was particularly pronounced, with the virus concentration in the first permeate sample obtained after a 10 min disruption being nearly 3-orders of magnitude larger than that in the sample immediately before the disruption. In several cases, the virus concentration in the grab sample from the filtrate exceeded that in the feed solution, corresponding to a negative value of the LRV, which is a direct result of the release of large numbers of previously captured virus during the process disruption.

The experimental data were effectively analyzed using the internal concentration polarization model presented by Jackson et al[7] that accounts for virus capture and accumulation within the virus filter along with the release of previously captured virus during a process disruption. The virus sieving coefficient, a measure of the rate at which the accumulated (mobile) virus leave the reservoir zone, was found to be relatively insensitive to the operating conditions, with all of the data well-described using $S = 1.2 \times 10^{-4}$. However, the fraction of virus that are captured upon entering the PVDF membrane increased from 90.1% to 99.8% as the filtrate flux increased from 5 to 120 L/m^2/h. In addition, the fraction of virus released during the process disruption was a strong function of the duration of the disruption, varying from less than 5% for a 2 min disruption to 100% for disruption times ≥30 min. This behavior is consistent with previous

studies suggesting that virus diffusion enables the previously captured virus to escape from their trapped position in the absence of the filtrate flow.

In contrast to previous studies, data obtained using an extensive buffer flush after a short virus challenge showed a bi-phasic decay in the virus concentration over more than 1500 L/m^2 of buffer. This bi-phasic behavior has not been reported previously since it can only be observed when performing a prolonged buffer flush. This bi-phasic response could be accurately modeled by assuming that the reservoir (or capture) zone in the PVDF membrane consisted of two different regions (or pathways), each with a different virus sieving coefficient. In this case, the more retentive region has a sieving coefficient of $S_2 = 1.1 \times 10^{-5}$, an order of magnitude smaller than the sieving coefficient through the more permeable zone. This behavior could well arise from inhomogeneities in the pore size distribution within the PVDF membrane. Future studies will be required to determine the generality of this result with other virus filters, including those with highly asymmetric pore structures, as well as the dependence of the model parameters on the properties of both the virus (e.g., size and charge) and the filtration membrane.

ACKNOWLEDGMENTS

This work was supported through the Membrane Science, Engineering, and Technology (MAST) Center, which is funded by grant number 1841474 from the NSF IUCRC program. The authors would also like to thank Seon Yeop Jung, Natalie Thompson, and Matthew Curtis for their assistance in the propagation of bacteriophage and the development of the plaque assay.

CONFLICT OF INTEREST

The authors declare no conflict of interest.

AUTHOR CONTRIBUTIONS

Mohammad A. Afzal: Data curation (lead); formal analysis (equal); investigation (lead); writing – original draft (lead). **Andrew L. Zydney:** Conceptualization (lead); formal analysis (equal); funding acquisition (lead); methodology (lead); project administration (lead); supervision (lead); writing – review and editing (lead).

DATA AVAILABILITY STATEMENT

Data available on request from the authors.

ORCID

Andrew L. Zydney https://orcid.org/0000-0003-1865-9156

REFERENCES

1. Kiss RD. Practicing safe cell culture: applied process designs for minimizing virus contamination risk. *PDA J Pharm Sci Technol*. 2011;65:715-729.
2. Lieber MM, Benveniste RE, Livingston DM, Todaro GJ. Mammalian cells in culture frequently release type C viruses. *Science*. 1973;182(80):56-59.
3. FDA. Points to consider in the manufacture and testing of monoclonal antibody products for human use. *J Immunother*. 1997;20(3):214-215.
4. EMEA. *Note for Guidance on Plasma-Derived Medicinal Products*. European Medicines Evaluation Agency; 2001.
5. Bolton GR, Cabatingan M, Rubino M, Lute S, Brorson K, Bailey M. Normal-flow virus filtration: detection and assessment of the end-point in bioprocessing. *Biotechnol Appl Biochem*. 2005;42:133-142.
6. Lute S, Bailey M, Combs J, Sukumar M, Brorson K. Phage passage after extended processing in small-virus-retentive filters. *Biotechnol Appl Biochem*. 2007;47:141-151.
7. Jackson NB, Bakhshayeshi M, Zydney AL, Mehta A, van Reis R, Kuriyel R. Internal virus polarization model for virus retention by the Ultipor® VF grade DV20 membrane. *Biotechnol Prog*. 2014;30:856-863.
8. Strauss D, Goldstein J, Hongo-Hirasaki T, et al. Characterizing the impact of pressure on virus filtration processes and establishing design spaces to ensure effective parvovirus removal. *Biotechnol Prog*. 2017;33(5):1294-1302.
9. Fan R, Namila F, Sansongko D, et al. The effects of flux on the clearance of minute virus of mice during constant flux virus filtration. *Biotechnol Bioeng*. 2021;118(9):3511-3521.
10. Yamamoto A, Hongo-Hirasaki T, Uchi Y, Hayashida H, Nagoya F. Effect of hydrodynamic forces on virus removal capability of Planova filters. *AIChE J*. 2014;60(6):2286-2297.
11. Dishari SK, Micklin MR, Sung K-J, Zydney AL, Venkiteshwaran A, Earley JN. Effects of solution conditions on virus retention by the Viresolve® NFP filter. *Biotechnol Prog*. 2015;31:1280-1286.
12. Dishari SK, Venkiteshwaran A, Zydney AL. Probing effects of pressure release on virus capture during virus filtration using confocal microscopy. *Biotechnol Bioeng*. 2015;112(10):2115-2122.
13. Lacasse D, Genest P, Pizzelli K, Greenhalgh P, Mullin L, Slocum A. Impact of process interruption on virus retention of small-virus filters. *Bioprocess Int*. 2013;11(10):34-44.
14. Woods MA, Zydney AL. Effects of a pressure release on virus retention with the Ultipor DV20 membrane. *Biotechnol Bioeng*. 2014;111(3):545-551.
15. LaCasse D, Lute S, Fiadeiro M, et al. Mechanistic failure mode investigation and resolution of parvovirus retentive filters. *Biotechnol Prog*. 2016;32:959-970.
16. Wu H, Cai Y, Schwartz DK. Particle remobilization in filtration membranes during flow interruption. *J Memb Sci*. 2020;610:118405.
17. David L, Niklas J, Budde B, Lobedann M, Schembecker G. Continuous viral filtration for the production of monoclonal antibodies. *Chem Eng Res Des*. 2019;152:336-347.
18. Leisi R, Widmer E, Gooch B, Roth J, Ros C. Mechanistic insights into flow-dependent virus retention in different nanofilter membranes. *J Membr Sci*. 2021;636:119548.

How to cite this article: Afzal MA, Zydney AL. Effect of filtrate flux and process disruptions on virus retention by a relatively homogeneous virus removal membrane. *Biotechnol. Prog*. 2022;38(4):e3255. doi:10.1002/btpr.3255